Construction and Building Materials 270 (2021) 121421

Contents lists available at ScienceDirect

Construction and Building Materials

journal homepage: www.elsevier.com/locate/conbuildmat

Effects of surface roughness and light scattering on the activation of TiO_2 on mortar photocatalytic process

Sérgio Roberto Andrade Dantas [a,b,*], Roberto Cesar de Oliveira Romano [a], Fúlvio Vittorino [b], Kai Loh [a]

[a] Polytechnic School of the University of São Paulo, Department of Civil Construction Engineering, 83 Prof. Almeida Prado Avenue, trav. 2, 05424-970 São Paulo, Brazil
[b] Institute of Technological Research of São Paulo, 532 Prof. Almeida Prado Avenue, 05508-901 São Paulo, Brazil

HIGHLIGHTS

- Activation of TiO_2 by diffuse/direct solar radiation.
- Relationship of different roughness scales with the dispersion/activation of TiO_2.
- Distinct particle sizes of TiO_2 and the formation of TiO_2 magnetic mesh.
- The TiO_2 magnetic mesh and photocatalysis system efficiency.
- The TiO_2 in suspension and the film layer activation effectiveness.

GRAPHICAL ABSTRACT

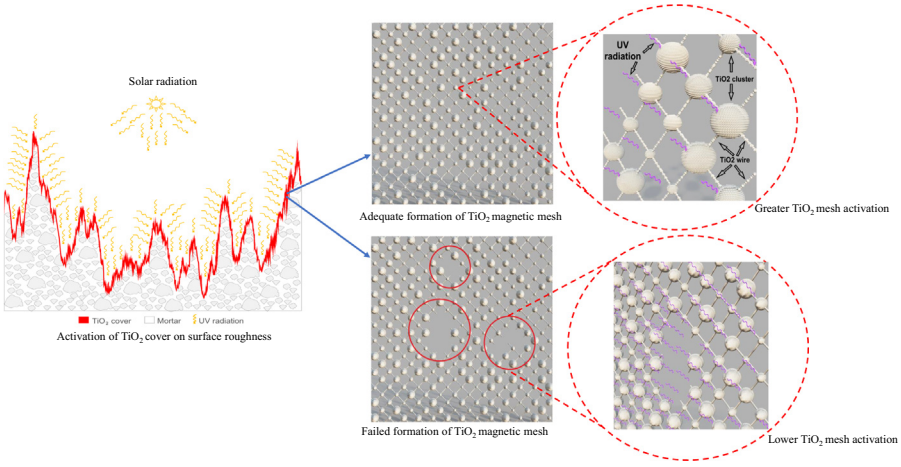

ARTICLE INFO

Article history:
Received 5 August 2020
Received in revised form 9 October 2020
Accepted 20 October 2020
Available online 15 November 2020

Keywords:
Mortar surface
Light scattering
UV light
TiO_2 activation
Photocatalysis

ABSTRACT

Purpose: To assess the effects of the activation of TiO_2 as a function of different roughness scales and light scattering on mortar surfaces.
Methods: Commercial samples of TiO_2 in powder and suspension form were compared using seven mortar samples with distinct treatments of TiO_2. Optical profilometer, Scanning Electron Microscopy, and EDS elemental mapping were used to evaluate the influence of roughness on the activation of TiO_2.
Conclusions: Activation of TiO_2 by diffuse solar radiation is as or more important than direct solar radiation; Micro-roughness has no direct relationship with the activation of TiO_2; The presence of different roughness scales and the use of the same particle size of TiO_2 affect the dispersion process of TiO_2; Different particle sizes of TiO_2 helped in the formation of TiO_2 magnetic mesh which improves system efficiency, and; Suspension of TiO_2 does not guarantee better effectiveness of the system due to imperfect film formation.

1. Introduction

TiO_2 nanoparticles (NPs) are commonly used in photocatalytic processes aiming to obtain self-cleaning surfaces [1–5], and, at the same time, the few investigations on TiO_2 microparticles

* Corresponding author at: Polytechnic School of the University of São Paulo, Department of Civil Construction Engineering, 83 Prof. Almeida Prado Avenue, trav. 2, 05424-970 São Paulo, Brazil.
E-mail address: sergiodantas@usp.br (S. Roberto Andrade Dantas).

https://doi.org/10.1016/j.conbuildmat.2020.121421
0950-0618/

(MPs) reinforce the idea of the low efficacy of larger particles for this purpose [6,7]. Among the factors that may influence photocatalytic activity, the following three are considered relevant: (i) the amount of photoactive TiO_2 particles (active sites) on the surface, (ii) particle size and morphology of TiO_2, and (iii) crystalline structure of TiO_2 [8,9].

The shape and particle size of TiO_2 are significant since photocatalytic activity depends on both [3]. Another point is that UV radiation is strongly absorbed, with the strongest visible light scattering power, at the particle size of TiO_2 of approximately 0.2 μm [10]. However, this could be applying well to spherical pigment particles separated by large distances compared to the light wavelength, but it is less useful when particles are packed [11].

The addition of TiO_2 powder on the cement matrix results in problems because it is introduced in the dry state, and it also has a strong tendency to form agglomerates; however, the efficiency of the photocatalytic activity can be increased if TiO_2 is applied as a suspension [12–14]. Considering that no real surface is perfectly smooth and no two rough surfaces are identical [15], surface roughness can affect how TiO_2 particles can be activated by solar radiation incidence, which can lead to a micro-shading effect in TiO_2 particles caused by the different roughness scales existing on surfaces.

The extent to which surface roughness affects wave scattering becomes important when the scattering properties of a surface strongly depend on a range of roughness scales around the wavelength of the incident wave and when a rough surface exhibits more than one scale of roughness [15]. Therefore, the modern nanotechnology considers that surfaces roughness need to improve the study of interactions at the nano- and microscales [16].

Rough surface measurement techniques generally are classified as contact and non-contact methods, and, in general, a minimum of two surface parameters is needed to characterize a rough surface: a height and a spatial parameter [17]. However, the difficulties associated with rough surface measurement arise from the nature of the surface, once roughness is not an intrinsic surface property and depends on sample length and the sampling interval used [15].

This study discusses the effects of the form of application of TiO_2 –powder and suspension – on the activation of TiO_2 as a function of roughness surfaces using an optical profilometer, Scanning Electron Microscopy, EDS elemental mapping, and the electromagnetic wave theory to understand how the phenomenon of light reflection occurs and the influence of roughness on photocatalytic activity considering the different roughness scales of mortar surfaces.

This research does not present what would be the best procedure for the use of TiO_2 if added in the cement matrix or applied as a suspension since both methods have limitations that hinder the activation of TiO_2 by UV light. However, TiO_2 must have a particle size that allows a good dispersion forming the cake cover. In other words, these particles can be activated by solar radiation (direct or diffuse) at the time of the incidence of UV light, thereby limiting the influence of micro-shading and pollution particles on this activation and, consequently, causing a more effective photocatalysis process.

2. Material and methods

This research observed the effects of the activation of TiO_2 as a function of different roughness scales and light scattering on mortar surfaces with distinct treatments of TiO_2 –either in powder and suspension form. Thus, an experimental program was developed in which samples were observed at different scales, with an observation path from the larger scale to a more refined scale using optical profilometry tests to observe the surface microscopic distribution, passing to scanning electron microscopy (SEM) to identify the morphology and formation of TiO_2 film from the suspensions, and finally, arriving at EDS elementary mapping to observe the presence and dispersion of TiO_2 powder when added in mortar.

2.1. Experimental design

Commercial samples of TiO_2 in powder and suspension were compared using seven mortar samples with distinct treatments of TiO_2. The P25p and PC105p powder form was added to the cement matrix after being pre-dispersed in water. The P25s and PC105s are suspensions prepared by the author in the laboratory using High Energy of Dispersion (HED), while PC-S7s and E502s are commercial suspensions. All suspensions were applied as a spray to the surfaces of specimens, as recommended by the manufacturer, as well as the paint in the painted specimens so that the same application pattern could be maintained.

The experimental design compared four suspension samples of TiO_2 with two powder samples of TiO_2. Because of the dimensions and exposure conditions of the specimens, mortar samples are compared in pairs, while the reference has three samples to participate in each group. The specimens are divided into three groups (1–3) and assembled according to logic: G1 - comparing the same samples of TiO_2 powder and suspensions prepared in the laboratory; G2 - comparing different samples of TiO_2 powder with different commercial suspensions of TiO_2, and; G3 - comparing all samples of TiO_2 in suspension form, as described in Table 1. The final design of the specimens, which were exposed to solar radiation, is shown in Fig. 1.

2.2. Materials characterization

The characteristics of the raw materials are presented in Table 2. The specific surface area, real density, particle size of TiO_2, and particle size distribution of dolomite were determined accord Dantas et al. [18]. Fig. 2 presents the particle size distributions of materials.

According to Table 2 and Fig. 2, two points can be considered essential for understanding the relationship of TiO_2 with the roughness measured and its potential activation by UV radiation: specific surface area and particle sizes presented by each TiO_2 type. It is known that the smaller the particle size of TiO_2, the larger its specific areas and the greater the tendency to agglomerate. Consequently, there are more dispersion problems for the material on a very rough surface, as well as its activation through solar radiation, either on a surface containing TiO_2 in its matrix or covered by a film, as will be shown further in this study.

Fig. 3 shows the mineralogical compositions of the commercial powder samples (P25 and PC105) and suspension samples (PC-S7 and E502) of TiO_2 determined by X-ray diffraction, and Table 3 presents the amount of rutile and anatase quantified using the Rietveld method.

Table 4 shows the chemical composition of samples of TiO_2 determined by semiquantitative chemical analysis by X-ray fluorescence (XRF)[1,2]: Procedure IPT15101-CT-WORKS-LMCC-Q-PE-087 - Revision 0 of 03/28/2014 “Qualitative, semi-quantitative, or quan-

[1] For liquid samples, a Panalytical X-ray fluorescence spectrometer model Minipal Cement was used; using a sample holder with a 3.6 μm polyester x-ray film, the test was determined on the "in nature" sample. The semi-quantitative results are estimated by the manufacturer's internal standards and the curve called "OMNIAN".

[2] For solid samples, a Panalytical X-ray fluorescence spectrometer, Minipal Cement model was used from inserts fused in a Claisse model M4 fusion machine, using mixture fluxes of lithium tetraborate/lithium metaborate, brand MAXXIFLUX (66.57% Li2B4O7, 32.73% LiBO2 and 0.70% LiBr), with a proportion of 0.5 g of sample and 6.75 g of fondant. The semi-quantitative results are estimated by the manufacturer's internal standards and the curve called "OMNIAN" and they have been normalized to 100%.

Table 1
Description of the specimens.

Group	Mortar (painted)	Mortar (unpainted)	Mortar (unpainted)	Mortar (unpainted)	Mortar (unpainted)
G1	Ref.	P25p	PC105p	P25s	PC105s
G2	Ref.	P25p	PC105p	PC-S7s	E502s
G3	Ref.	P25s	PC105s	PC-S7s	E502s

Note: p = Powder / s = Suspension.

Fig. 1. Design and exposure to solar radiation of specimens.

Table 2
Characteristics of the raw materials.

Material	Particle Size (μm)			Specific surface area	Average density
	d_{10}	d_{50}	d_{90}	(m^2/g)	(cm^3)
White Portland cement	2.6	17.7	19.5	0.86	3.05
Dolomite #20	975	1242	1620	0.16	2.90
Dolomite #40	24.3	230	740	0.56	2.94
Dolomite #80	4.5	38.3	134	0.80	2.81
TiO_2 (P25 – powder)	1.38	3.90	17.7	49.4	3.84
TiO_2 (PC105 – powder)	0.66	1.50	4.60	79.8	3.62
TiO_2 (PC-S7 - suspension)	0.06	0.09	0.12	70.7	–
TiO_2 (E502 – suspension)	4.09	8.60	17.25	0.82	–

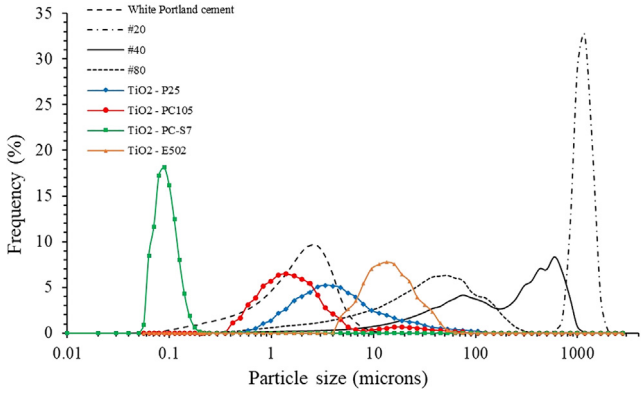

Fig. 2. Particle size distribution of materials.

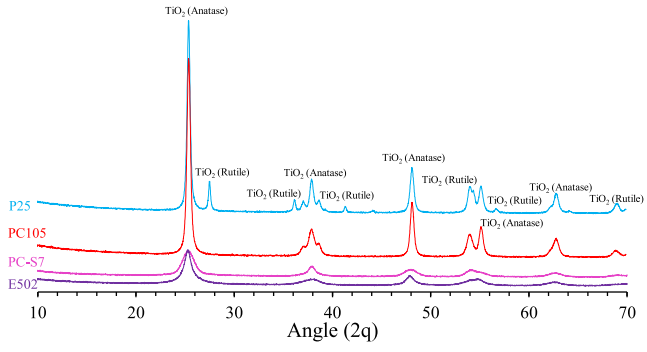

Fig. 3. X-ray diffractograms of samples of TiO_2.

titative chemical analysis by X-ray fluorescence spectrometry", in accordance with the Brazilian Association of Technical Standards (ABNT) [19].

Fig. 3 and Table 3 show that, except for the TiO_2-P25 sample, all other samples have the same crystalline phase. The crystalline phases of TiO_2 have a direct relationship with the band gap energy,

Table 3
Phases observed in TiO_2 and amount of rutile and anatase.

Sample	Phase	ICSD code	%
PC105	Anatase	93,098	100
P25	Anatase / Rutile	202,243 / 51,938	87.8 / 12.2
PCS7	Anatase	82,080 / 202,243	29.5 / 70.5
E502	Anatase Nanocrystaline	154,602	100

Table 4
Chemical composition of samples of TiO_2 by XRF.

Compound	P25 (%)	PC105 (%)	PC-S7 (%)	E502 (%)
TiO_2	99.7	99.6	96.1	90.6
SiO_2	0.25	–	0.21	1.17
Al_2O_3	–	0.12	0.09	0.46
FeO_3	0.02	0.03	–	–
CaO	–	–	0.14	1.21
MgO	–	–	0.20	0.64
P_2O_5	–	–	2.77	4.28
ZrO	–	0.03	0.04	–
Nb_2O_5	–	0.26	0.41	–
CdO	–	–	0.13	–
V_2O_5	–	–	–	1.56
CuO	0.02	0.03	–	–
Er_2O_3	–	0.10	–	–

being it 3.2 eV for the anatase phase and 3.0 eV for the rutile phase, therefore responsible for absorption and activation by solar radiation, as will be discussed later.

Table 4 shows that, concerning chemical compositions, TiO_2 powders (P25 and PC105) have greater purity than suspensions (PC-S7 and E502), the latter being of lower concentration but which cannot be associated with a lower photodegradation power when evaluated under the photocatalysis aspect.

2.3. Mortar composition

Compositions were developed without granulometric changes of coarse particles and the consumption, in kg/m^3, of each material is described in Table 5.

2.4. Setup of mixing and application process

The mixing procedure to prepare the mortar samples and suspensions is described below. Mortars were prepared and applied by a mason on specimens with dimensions of 1.2 m × 1.2 m as described by Dantas, Vittorino, and Loh [20]. Figs. 4–6 show the mixing and application in situ.

- Reference mortar: water was added to the construction mixer, and then microfibers were added. Mixing was performed for 5 min; after that, the dry powder was added, and 1 min was allowed for particle wetting. Hereafter, mixing was performed for more than 5 min.
- P25p and PC105p mortar: water was added to the construction mixer, and then microfibers were added. Mixing was performed for 5 min; after that, TiO_2 powder was added for 1 min, followed by all the dry powder, and 1 min was allowed for particle wetting. Then, mixing was performed for more than 5 min

Table 5
Consumption, in kg/m^3, of each raw material.

Material	Ref. [1]	P25p	PC105p	P25s[2]	PC105s[2]	PC-S7s[2]	E502s[2]
White Portland cement	115.1	114.1	114.1	115.1	115.1	115.1	115.1
Dolomite # 20	67.3	66.7	66.7	67.3	67.3	67.3	67.3
Dolomite # 40	378.4	375.1	375.1	378.4	378.4	378.4	378.4
Dolomite # 80	104.1	103.2	103.2	104.1	104.1	104.1	104.1
Water retainer	1.5	1.5	1.5	1.5	1.5	1.5	1.5
Air entrainment	0.2	0.2	0.2	0.2	0.2	0.2	0.2
Water	332.0	365.2	349.1	332.0	332.0	332.0	332.0
Polypropylene microfibers	1.5	1.5	1.5	1.5	1.5	1.5	1.5
TiO_2 (P25)	–	4.5	–	0.5	–	–	–
TiO_2 (PC105)	–	–	4.8	–	0.5	–	–
TiO_2 (PC-S7)	–	–	–	–	–	**	–
TiO_2 (E502)	–	–	–	–	–	–	***

Note: Specimens painted by spray after 28 days of mortar application (1); Suspensions applied by spray after 28 days of mortar application (2); Spray Rate: 15 m^2/ L (**); Spray Rate: 10 m^2/ L (***).

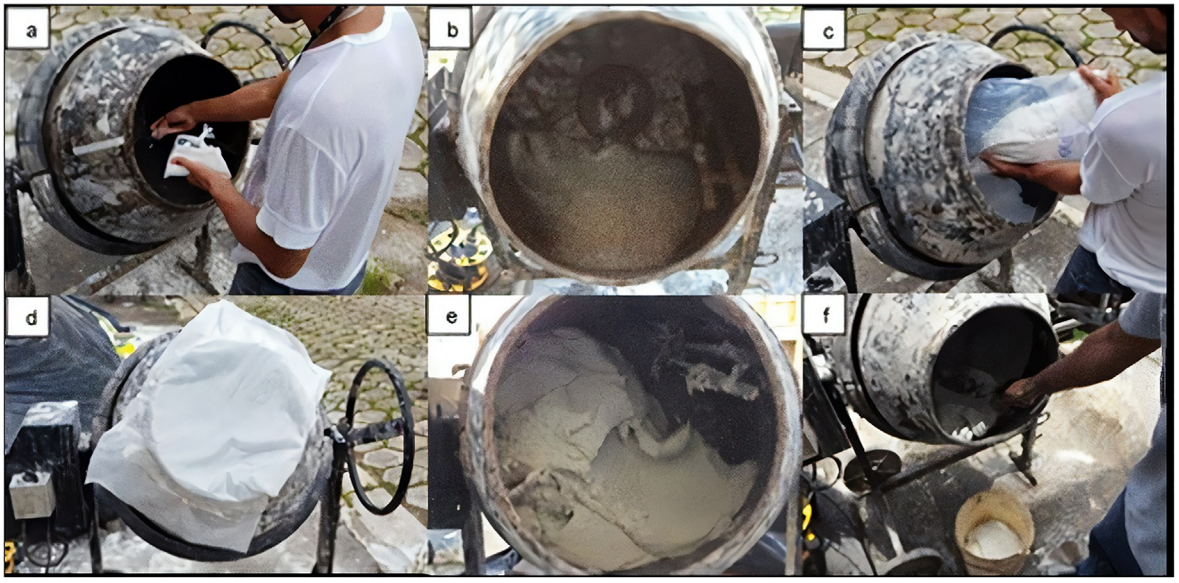

Fig. 4. Mixing mortar setup. Addition of microfibers and mixing (a - b); Addition of TiO_2 (c); particle wetting (d); mixing of mortar (e - f).

Fig. 5. Mortar application by mason in situ.

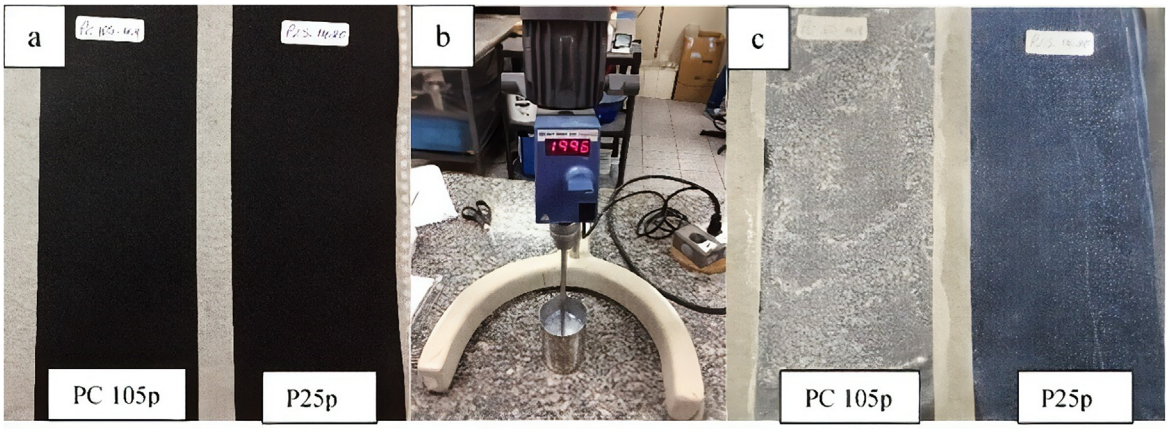

Fig. 6. PP surfaces before suspension impregnation (a); HED equipment (b); suspension impregnation after HED (c).

- P25s and PC105s suspensions were prepared in laboratory based on the results of the total solid residues of PC-S7s and E502s suspensions. The quantity equivalent to 14.4 g for each powder sample (P25p and PC105p) was mixed with 100 ml of deionized water using HED (2000 rpm with cowles propellant) for 5 min. After that, the suspensions were applied on black polypropylene (PP) plastic surfaces to observe adhesion.

2.5. Surface characterization

The parameters used to describe the rough surface depend only on the sampling length and instrument resolution [21]. In this study, an optical profilometer (non-contact method), Scanning Electron Microscopy (SEM), and EDS elemental mapping were used to surface characterization.

The shape and structure of seven different mortar samples with an area of 10 mm × 10 mm were analyzed employing eight measurements for each mortar sample by laser interferometry using a Bruker NPFLEX™ optical profilometer according to the following parameters: 5x objective lens (Michelson) with green monochrome light and 2x multiplier factor, measured area x = 623.4 μm and y = 467.5 μm and interval sampling of 0.974 μm, scan speed equal to 5x and noise limit (valid pixels) of 1%, and distance in "z" equal to 800 μm.

The measurements by optical profilometer allowed the creation of Gaussian distributions for each of the eight measurements. From these Gaussian distributions, assuming normal distribution, defined by the mean and variance values of each measurement, an equivalent normal curve for each sample was created from the linear combination of the results obtained from these eight measurements. The result is expressed in terms of probability density, which allows the comparison of the equivalent curves for each of the samples. To confirm and understand the equivalent curves found, variation coefficient was applied for the mortar samples.

The mortar samples were characterized using the FEI Quanta 3D FEG scanning electron microscope (SEM) and the elemental microanalysis by EDAX detector, Genesis version. Mortar samples were sectioned with a dry diamond saw and impregnated in vacuum by epoxy resin and polished with silicon carbide and diamond paste to obtain a smooth surface. A control mortar sample, without impregnation, was used to compare the surfaces where TiO_2 was added. All mortar samples were covered with gold and an electron

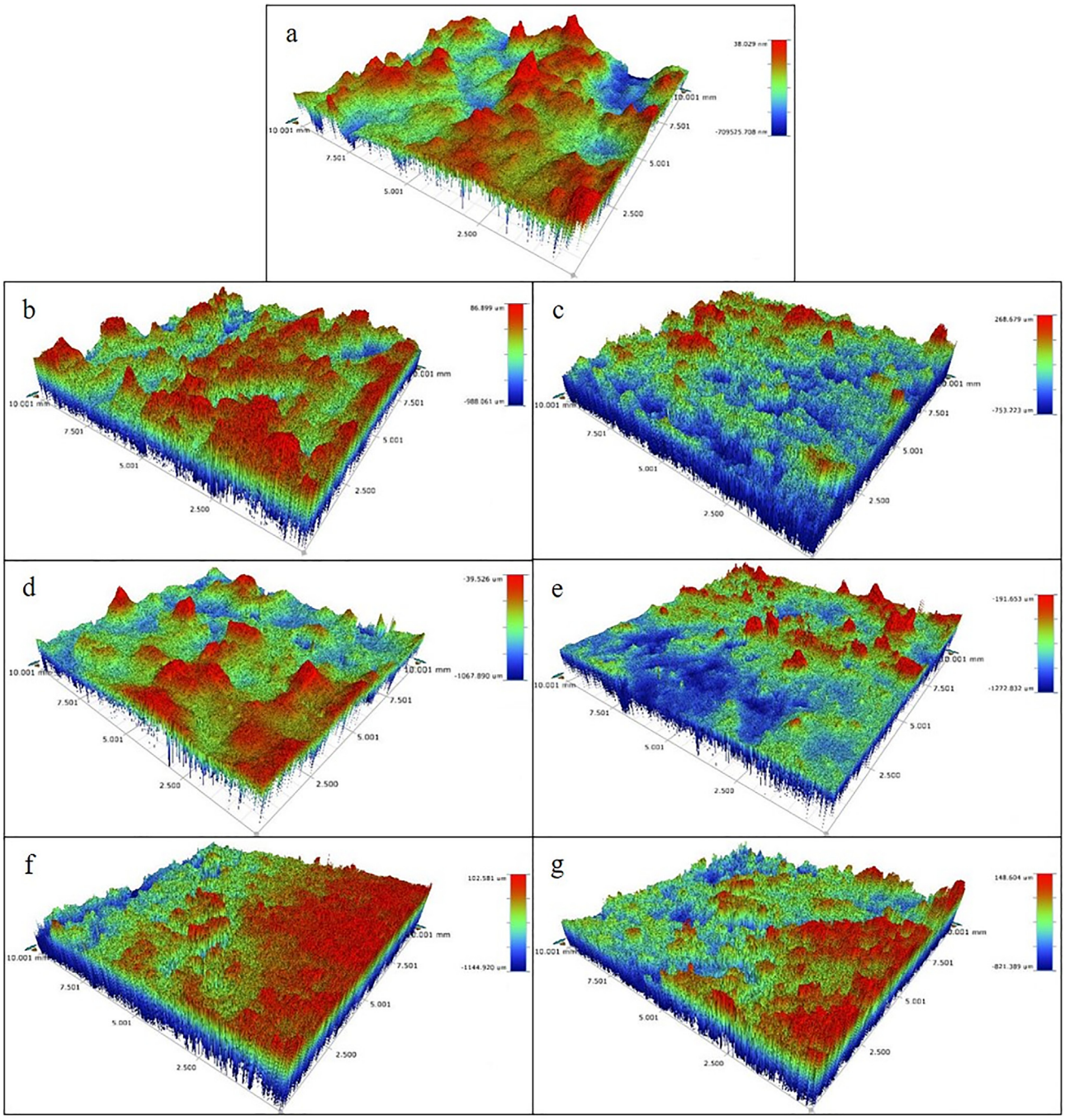

Fig. 7. Surface topography of specimens. Ref_painted (a); P25p (b); PC105p (c); P25s (d); PC105s (e); PC-S7s (f); E502s (g).

backscatter detector was used to better contrast the light and heavy elements. The voltage used was 20 kV and the working distance (WD) was approximately 10 mm.

In order to confirm the P25p and PC105p dispersion on the surfaces of mortar samples, EDS elemental mapping was done. The EDS map was made using a Thermo detector by Noran system (SIX) and the images obtained with a secondary electron detector (SEI) using a JEOL-JSM 6300 scanning electron microscope. Mortar samples were metalized with Au / Pd for 120 s and fixed on a microscope sample holder at four different points: (i) top layer, corresponding to the exposed surface; (ii) upper layer (≈2 mm); (iii) middle layer (≈50 mm), and; (iv) bottom layer (≈100 mm). An acceleration voltage of 20 kV and magnification of 50x was used with an image acquisition of approximately 1 h.

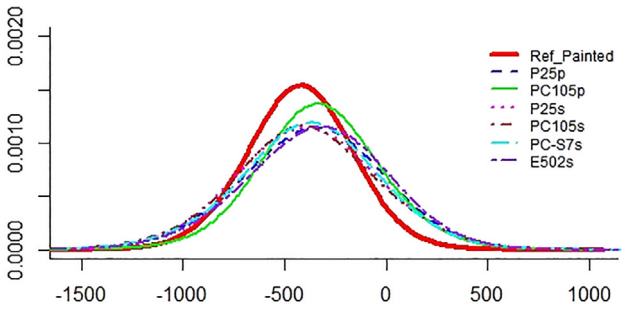

Fig. 8. Surface normal distribution.

Table 6
Variation coefficient of mortar samples.

Material	Ref.	P25p	PC105p	P25s	PC105s	PC-S7s	E502s
Equivalent average	−397	−378	−332	−380	−364	−347	−343
Equivalent variance	8012	14,718	10,793	15,067	11,250	13,872	13,858
Equivalent standard deviation	90	121	104	123	106	118	118
Coefficient of variation*	23%	32%	31%	32%	29%	34%	34%

Note: * values are shown in module.

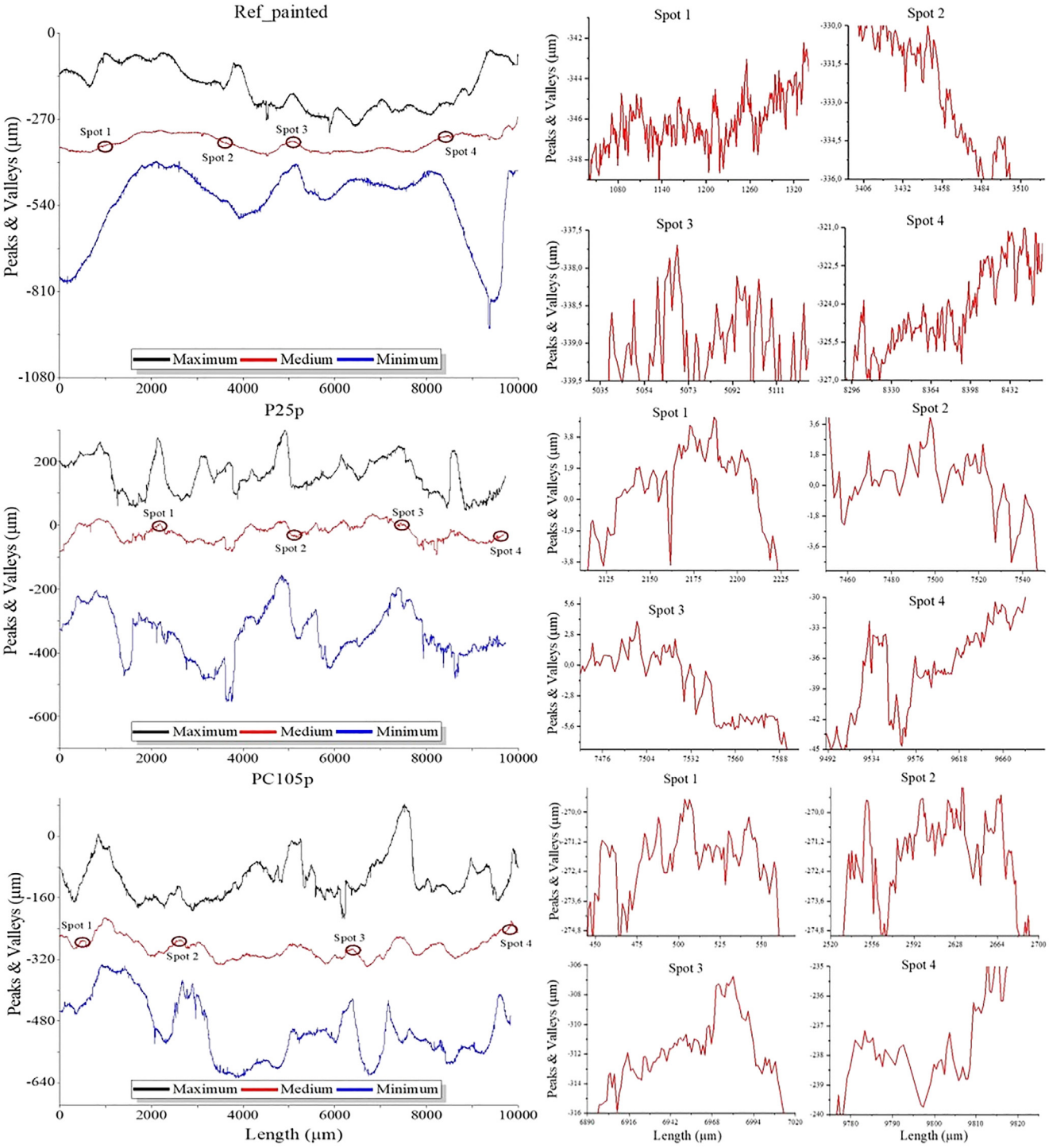

Fig. 9. Roughness profile and spot details: Ref_painted, P25p, and PC105p mortar samples.

3. Results

3.1. Surface characterization

3.1.1. Surface topography (profilometer)

Average roughness for each mortar sample is shown in Fig. 7 and proves that, despite the same base of composition and same operator being used, the specimens presented different roughness levels, which demonstrates the phenomenon of random roughness resulting from variation in the application process even when produced in similar ways.

One known model of roughness assumes that the roughness profile follows a Gaussian process with some correlation function [16]. However, a surface with exponential correlations may be misrepresented as a surface with Gaussian correlations because of the sampling interval used [22]. Thus, when considering height parameters to define the roughness of mortar samples, although no normality test has been applied, the curves apparently present a normal distribution, as shown in Fig. 8.

According to the graph, because of the amplitude (height) of the curves, it is possible to observe that the only specimens with significant roughness differences are Ref_painted and PC105p. On the other hand, the other samples could be considered virtually equal, as shown by the values of the coefficients of variation (CV) in Table 6.

Should be noted that, although the PC105p sample has a higher CV than the PC105s sample, when evaluating the standard deviation, it is observed that the PC105p sample has a lower value and, therefore, a curve more closed and higher than the PC105s sample. This is because the PC105s sample has higher averages than the PC105p sample, which leads to a higher standard deviation and consequent lower CV, and it is shown tangled with the other samples in the graph.

Roughness profiles were made using the values for the X-axis of all measurements taken for each mortar sample and represent what could be considered the maximum, medium, and minimum roughness for each specimen at the beginning of the urban environment exposure.

The results demonstrate the differences in amplitudes (peaks and valleys) between all mortar samples when evaluating the maximum, medium, and minimum roughness. Except for the P25p mortar sample, which presented maximum roughness in a positive scale, the other mortar samples presented negative values in their scales, with a great variety of these scales when comparing profiles, which demonstrates the heterogeneity of mortar samples and the randomization process with roughness production, thus hindering the homogenization of the scales when presenting profiles as shown in Figs. 9–11.

Considering the peak and valley heights shown in the profiles, when applying the amplitude of −400 μm–400 μm in the P25p and PC105p profile mortar sample, for example, a roughness of less than 1 mm was observed. This scale seems a typical aggregate and impossible for human control with the naked eye. In other words, the operator will not be able to smooth or even equalize something intrinsic to the material, making it impossible to control the surface on these scales.

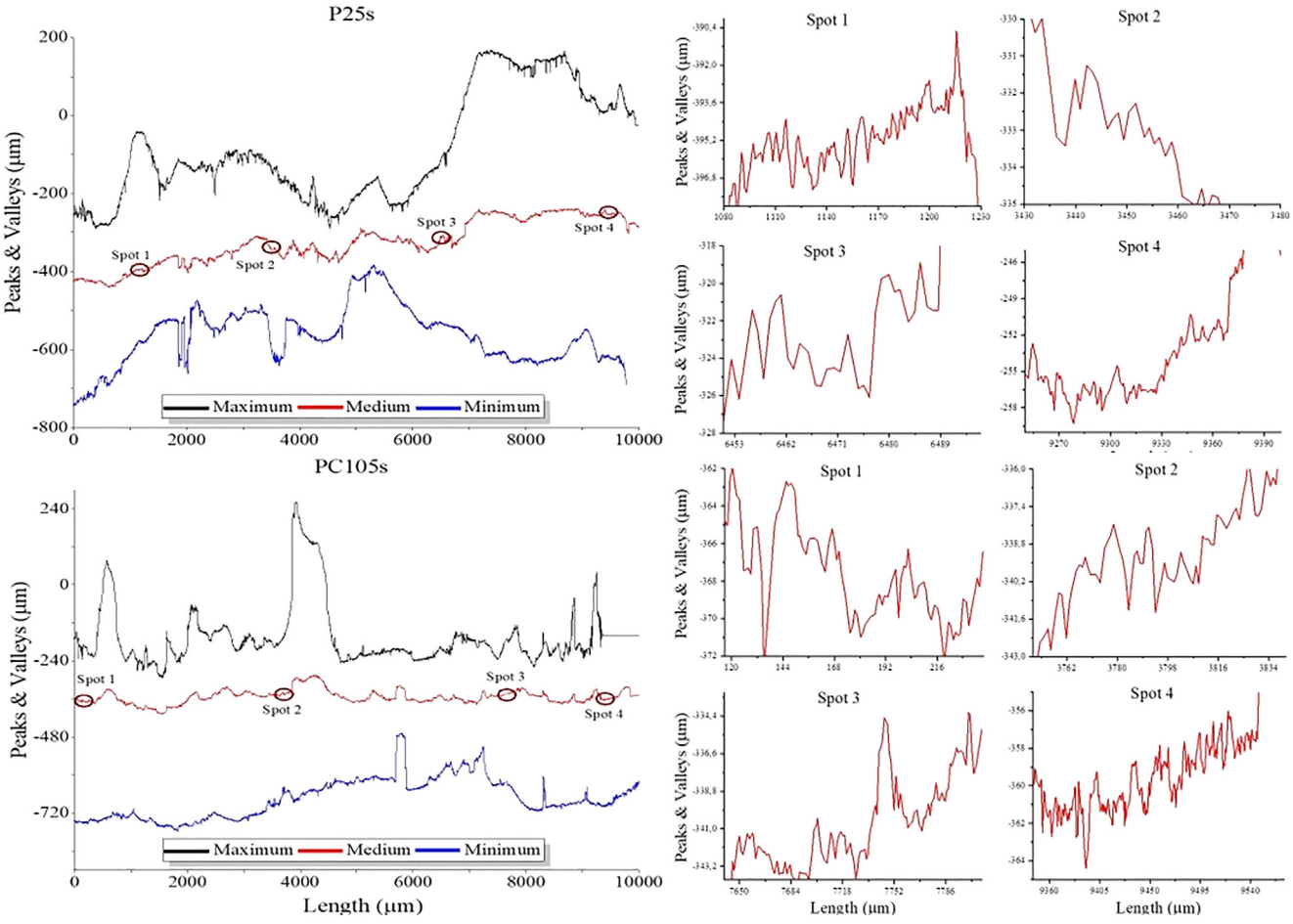

Fig. 10. Roughness profile and spot details: P25s and PC105s mortar samples.

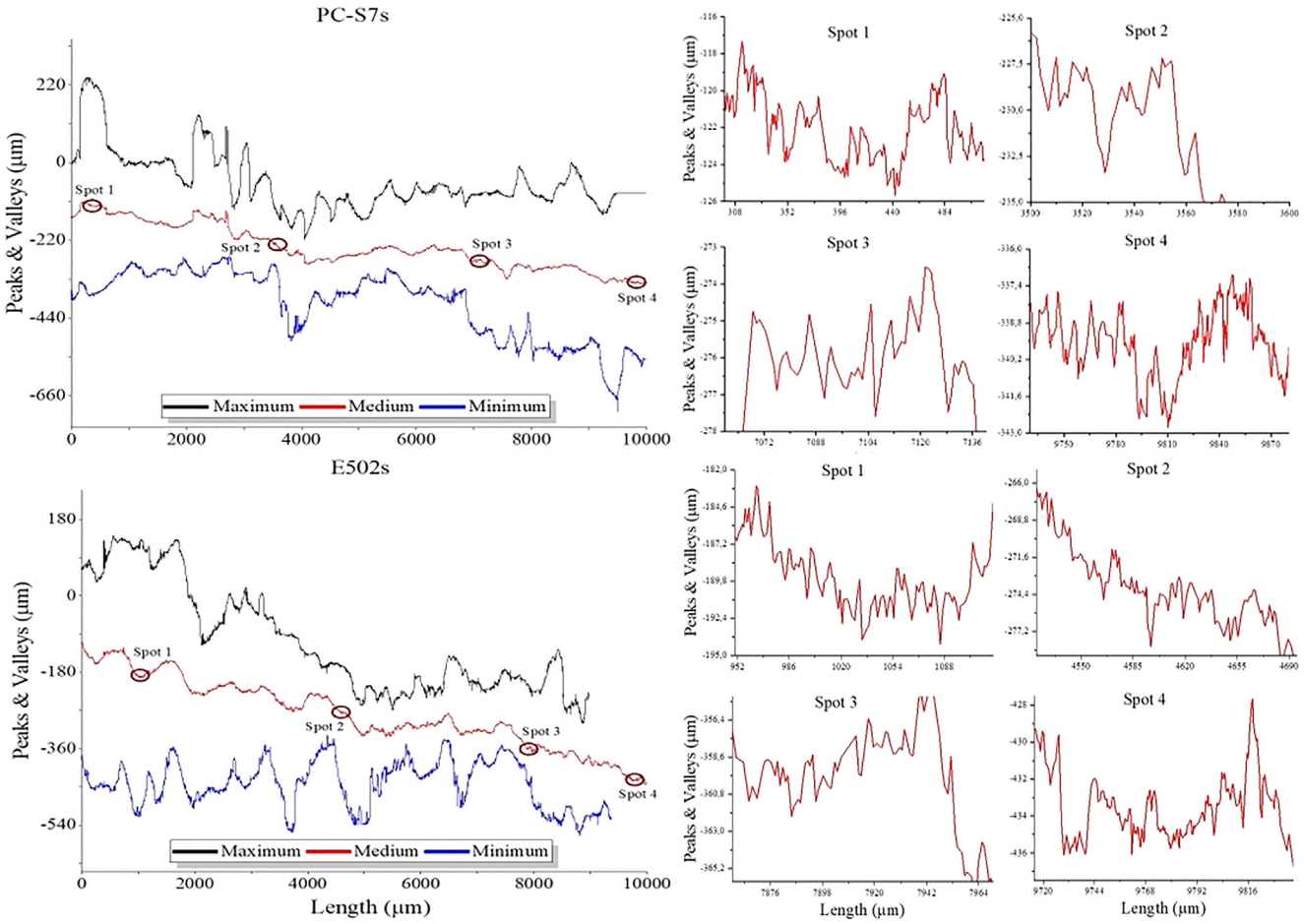

Fig. 11. Roughness profile and spot details: PC-S7s and E502s mortar samples.

Similarly, there is great variation for the spots from the medium roughness of each sample. It is possible to notice great heterogeneity when comparing the spots in the same mortar and much more when compared between the different samples. The micro-roughness found in these spots has a direct relationship with the dispersion of TiO_2 added to the mixture, as well as with the deposit of natural pollutants (dirt) on the surfaces of the specimens since they are exposed to the urban environment, which impacts the photodegradation process.

3.1.2. Scanning electron microscopy (SEM)

Regarding the measurements of each mortar surface by scanning electron microscope, for the P25p and PC105p mortar samples the roughness measured was of the mortar itself. On the other hand, for the Ref_painted, P25s, PC105s, PC-S7s, and E502s mortar samples, the roughness measured is not from only the mortar, but of the film layer caused by painting and by the TiO_2 suspension applied. The amplitude measurements in these profiles indicate the passage of the profilometer once on the film and once on the mortar, which shows the non-continuity of the film layer and the micro-roughness of the mortar and the film layer, respectively.

Moreover, the scanning electron microscope observations show that for Ref_painted, P25s, PC105s, PC-S7s and E502s mortar samples a film layer was formed, although not continuous as expected, which shows flawed spots on the films layers, as indicated by points (1) and (2) in the images. The other images allow the observation at other scales for a better understanding of the formation of a film layer in these surfaces, as show in Figs. 12–14.

Microscopic images demonstrate that in none of the surfaces where TiO_2 suspensions were applied the formation of a complete film layer could be observed, and the E502s suspension had the most homogeneous film layer, as can be seen in images 14e and 14f. All suspensions followed an application pattern recommended and specified by the manufacturer, in spray mode. However, it is important to remember that the incomplete formation of film layer considerably influence the photocatalysis process, since failures in their formations will not provide the correct activation of TiO_2.

Regarding the P25p and PC105p mortar samples, from the microscopy images, particle morphology could be observed added to the mixture. Despite that, when evaluating the dispersion of TiO_2 powder, the images did not identify good dispersion of TiO_2 as it presented large space between particles, which could be evaluated as the absence of TiO_2 in the surface of mortar samples. Particle morphology and mortar surfaces are identified by numbers (1) and (2), respectively. Other images allow the observation of particle morphology and dispersion at different scales, which brings a greater understanding on the dispersion of TiO_2 in these surfaces, as shown in Fig. 15.

3.1.3. Elemental mapping (EDS)

Despite the results found with electron microscopy, elementary mapping showed a higher P25p and PC105p concentration in the surface of mortar samples, as well as their distribution in lower layers, as shown in Fig. 16.

The mortar samples exhibit practically the same amount of TiO_2 in the top layer. However, PC105p presented more agglomeration

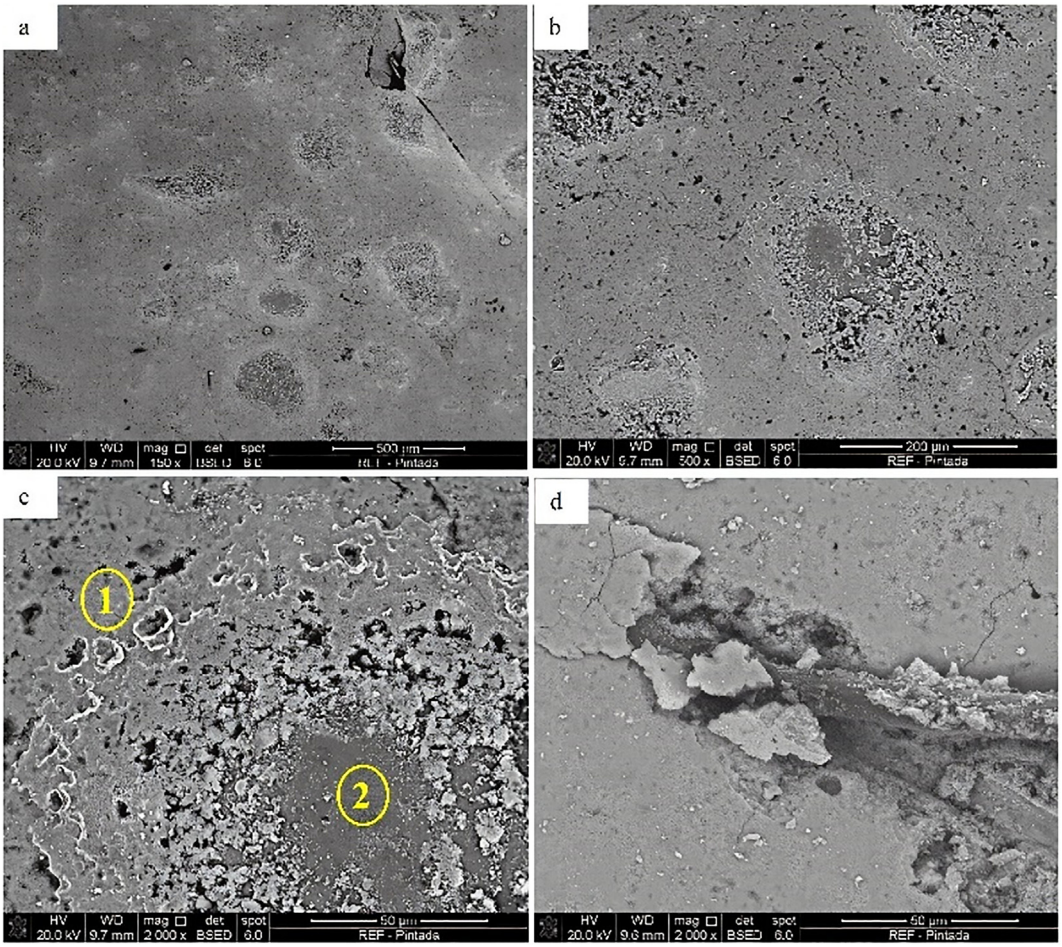

Fig. 12. Ref_painted mortar (a - d) Note: Paint film formation at 500 μm scale (a); Paint film formation at 200 μm scale (b); Paint film formation at 50 μm (1c); Paint film flawed spot at 50 μm (2c); Polypropylene microfibers at 50 μm scale (d).

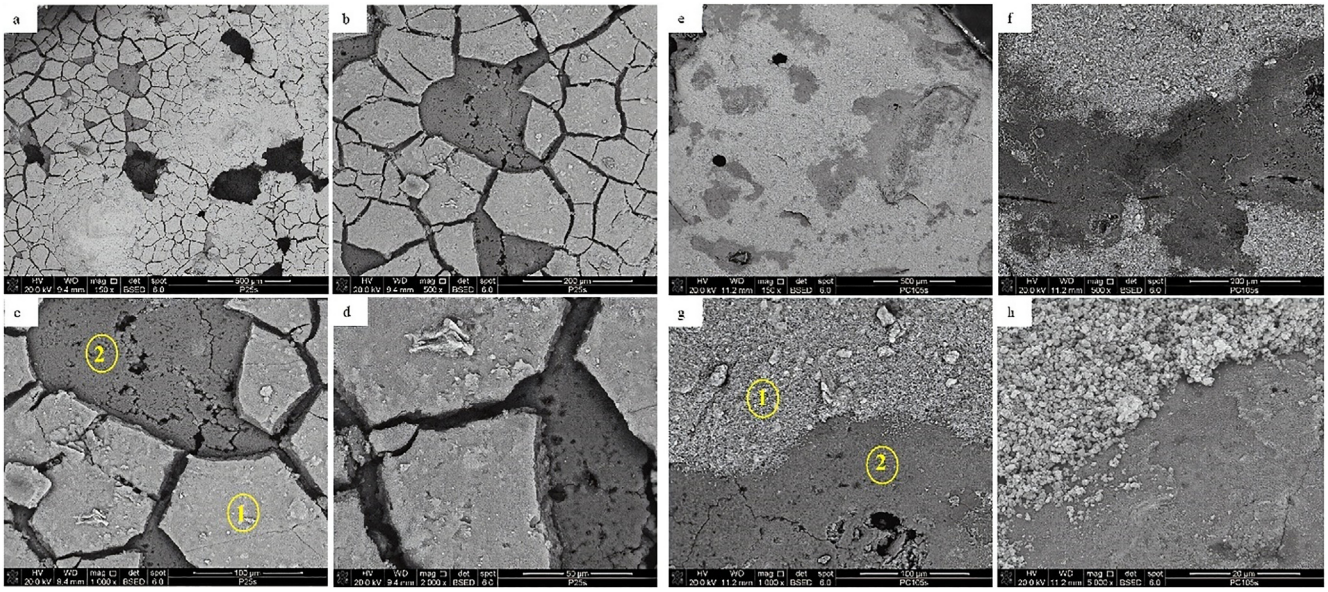

Fig. 13. P25s mortar (a - d); PC105s mortar (e – h) Note: Formation of TiO_2 film at 500 μm scale (a, e); Formation of TiO_2 film at 200 μm scale (b, f); Formation of TiO_2 film at 100 μm (1c; 1g); TiO_2 film flawed spot at 100 μm (2c, 2g); Formation of TiO_2 film at 50 μm (d); Formation of TiO_2 film at 20 μm (h).

areas, which was already expected considering the dimensions of its particles. Dispersion difference only begins to appear from the upper layer. The P25p sample reveals a high drop in the amount of particles in the upper layer, from 105 to 20 K, as shown in Fig. 16 (a – b), and the amount of particles remained practically the same in the middle and bottom layers, 26–27 K, as shown in

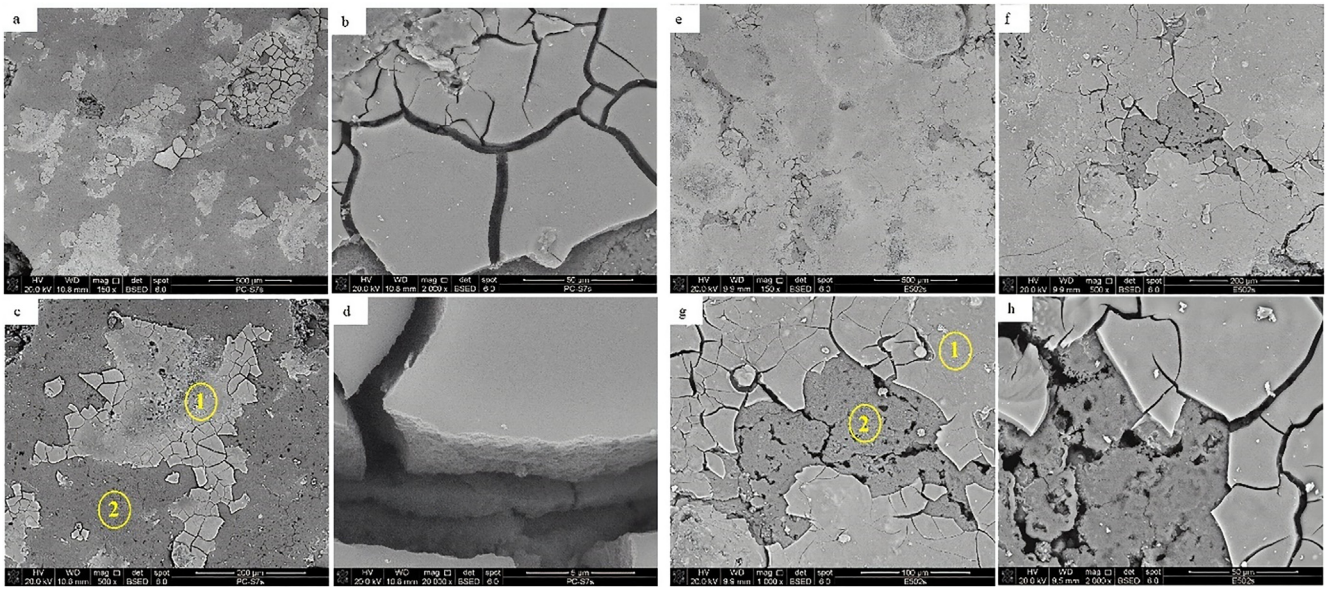

Fig. 14. PC-S7s mortar (a - d); E502s mortar (e – h) Note: Formation of TiO_2 film at 500 μm scale (a, e); Formation of TiO_2 film at 200 μm scale (f); Formation of TiO_2 film at 200 μm (1c); TiO_2 film flawed spot at 200 μm (2c); Formation of TiO_2 film at 100 μm (1g); TiO_2 film flawed spot in 100 μm (2g); Formation of TiO_2 film at 50 μm (b, h); Formation of TiO_2 film at 5 μm (d).

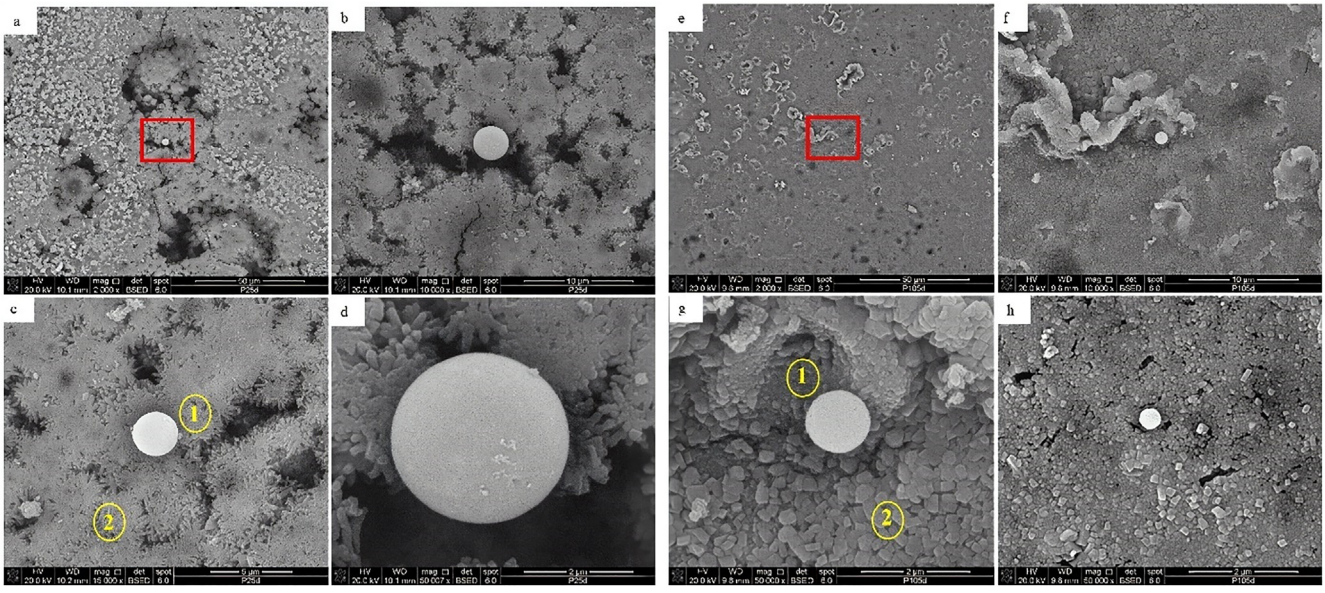

Fig. 15. P25p mortar (a - d); PC105p mortar (e – h). Note: TiO_2 particle dispersion at 50 μm scale (a, e); TiO_2 particle dispersion at 10 μm scale (b, f); Morphology of TiO_2 at 5 μm scale (1c); Mortar surface at 5 μm (2c); Morphology of TiO_2 at 2 μm scale (1g); Mortar surface at 2 μm (2g); Morphology of TiO_2 at 2 μm scale (d, h).

Fig. 16 (c - d). On the other hand, PC105p reveals a low drop in the amount of the particles in the upper layer, from 116 to 64 K, as shown in Fig. 16 (e - f), and the amount of particles remained practically the same in the middle and bottom layers, 19–21 K, as shown in Fig. 16 (g - h).

Another point is the dispersion of TiO_2 in the deep layers of mortar. Despite the decreased number of counts (K), P25p seems to maintain the same dispersion, while the dispersion seems to change in PC105p probably because the particles are more distant and, therefore, less likely to agglomerate in a smaller quantity.

These results highlight the dispersion of TiO_2 in mortar surfaces and also the possibility of natural replacement of the photocatalytic layer during the process of surface wear. In other words, as the top layer undergoes during the process of natural wear, it can be automatically replaced by the upper layer just below it, which has the same photocatalytic properties that make it a better performance surface.

4. Discussion

4.1. Dispersion of TiO_2 on the surface

Considering the micro-roughness scale, it is possible to think that a perfect dispersion of TiO_2 promotes a complete and homogeneous distribution of TiO_2 over the entire surface. This layer would provide a complete activation of TiO_2 and greater efficiency of the system regarding the photocatalytic activity.

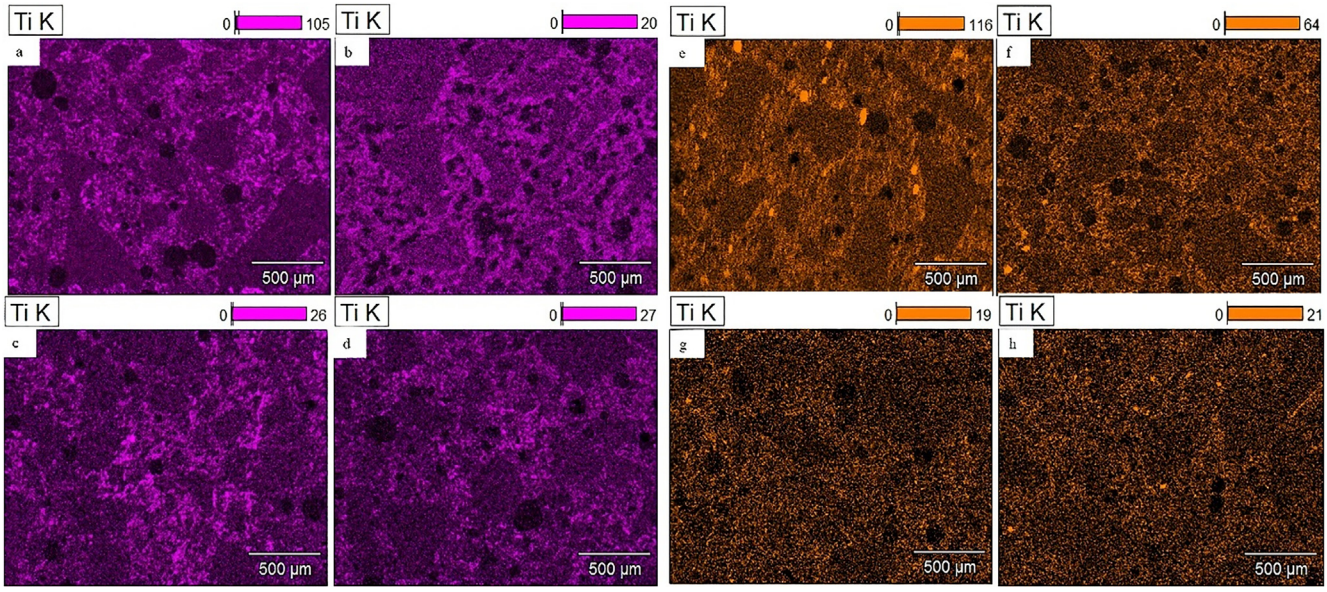

Fig. 16. P25p mortar (a - d); PC105p mortar (e – h). Note: Top layer (a); upper layer (b); middle layer (c); bottom layer (d). The colors are used to better differentiate between the two TiO_2.

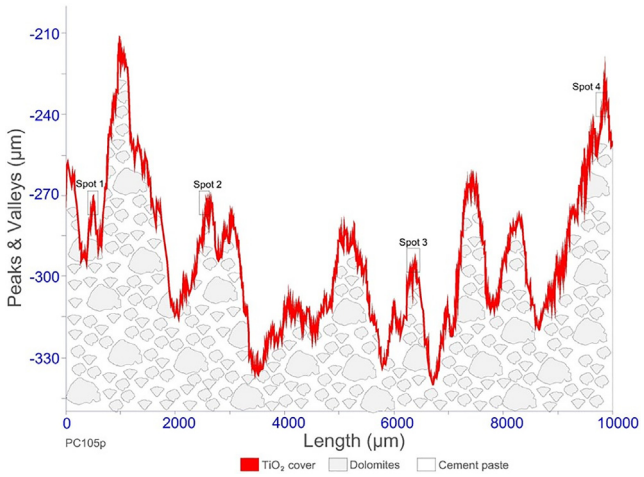

Fig. 17. Example of cake cover in the measured micro-roughness of the mortar sample with addition of TiO_2.

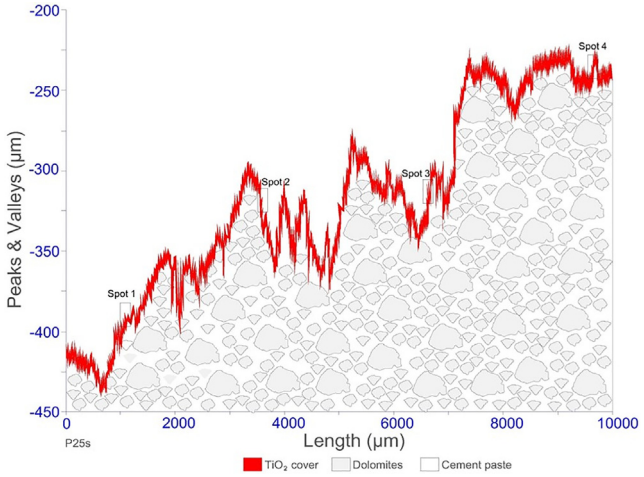

Fig. 18. Example of cake cover in the measured micro-roughness of the mortar sample with suspension of TiO_2.

This concept was considered in the roughness of mortar samples, which would create the idea about coverage that would represent a homogeneous distribution of TiO_2 as a functional cake cover, something that would seem like a film by the UV radiation but which is a magnetic network in the nano- and microscales. Therefore, considering a perfect dispersion in measured roughness, the red line in the surface of the PC105p and P25s mortar samples would be the representation of the cake cover to be found, since it is about a measured roughness, in other words, real surfaces, as shown in Figs. 17 and 18.

Surface evaluation on the degradation of atmospheric pollutants, considering that this surface is coated by the cake cover, leads to a scenario, at first, that the surface is completely covered by TiO_2 particles and pollution particles (PM10) above them. In a favorable situation, TiO_2 breaks the contact angles of PM10 and these particles can be carried away in the presence of rain, which provides the self-cleaning process.

However, not being a situation that can be guaranteed, some aspects could be considered: (i) TiO_2 will not be able to degrade the dirt deposited on the mortar with the same speed as the deposition, in other words, PM10 particles will deposit faster than TiO_2 can degrade them; (ii) if the smaller PM10 particle is deposited in the valleys, it would not be able to be carried away by the rain as it would be covered by other larger particles, and; (iii) considering the roughness, if there are TiO_2 particles deposited in the valleys and covered by PM10 particles, UV rays cannot reach these TiO_2 particles, and therefore, activate them.

Starting from this last hypothesis and observing all particle sizes involved in the process (PM = 10 µm and TiO_2 = 0.1 µm to 9 µm [d_{50}]), this makes it quite evident that PM10 particles easily cover all TiO_2 particles, as well as the surface where they are deposited, thus making a layer and preventing the activation of TiO_2. Hence, when thinking about the dispersion of TiO_2 particles over micro-roughness, it is also necessary to think about the dispersion of pollution particles in this same surface, which will use different roughness as an adhesion point.

Thereby, when considering the average diameters of the TiO_2 particles used in this study, as well as the characteristic diameter

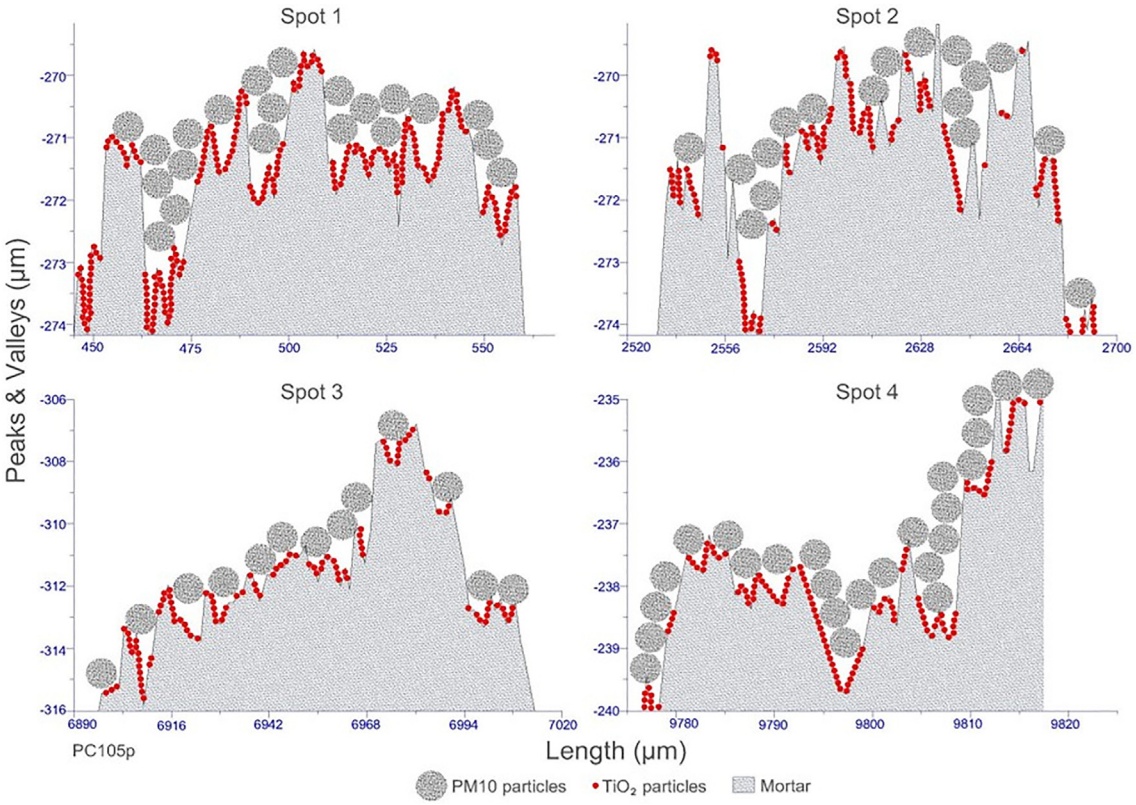

Fig. 19. Example of possible dispersion of TiO_2 (d_{50} = 1.5 µm) and PM10 (10 µm) in measured micro-roughness of the mortar sample with the addition of TiO_2.

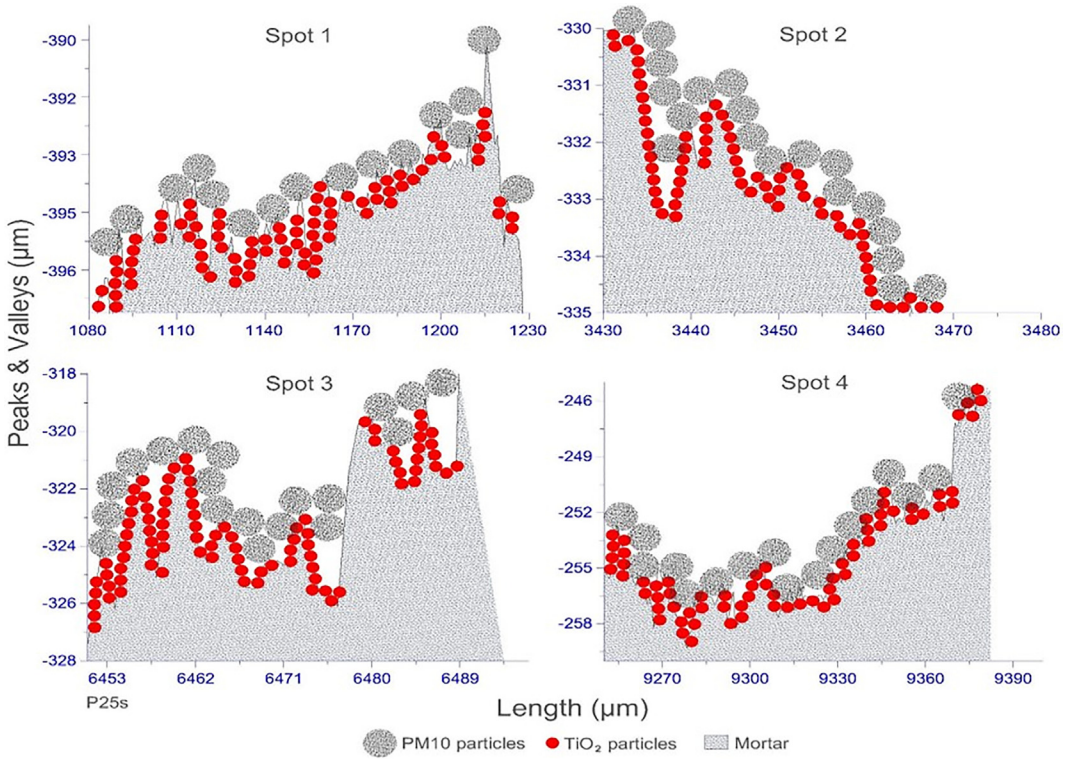

Fig. 20. Example of possible dispersion of TiO_2 (d_{50} = 3.90 µm) and PM10 (10 µm) in measured micro-roughness of the mortar sample with the suspension of TiO_2.

of the PM10 particles applied to the surfaces measured from the profilometer, it was possible to draw a probable dispersion for these particles in such surfaces. Thus, when evaluating the specific points of the average roughness of PC105p (d_{50} = 1.5 μm) and P25s (d_{50} = 3.90 μm) mortar, a probable dispersion of TiO_2 and PM10 particles (10 μm) is considered in each surface, which leads to a direct impact in the photodegradation of this pollutant with the non-activation of TiO_2 particles from their covering by PM10 particles, as shown in Figs. 19 and 20.

Therefore, in a micrometric scale, where the light interact with the surface and define light reflections, considering the existing micro-roughness, there would certainly be difficulties in the homogeneous activation of TiO_2 in surfaces, which would require, first, a partial PM10 degradation in the top layer that would allow the passage of UV rays to activate bottom TiO_2 particles and consequently a higher PM10 degradation.

4.2. Agglomerated or dispersed TiO_2?

In general, the literature assumes that the more dispersed the particles, the better the effect of TiO_2. However, it is important to point out some items in this discussion about what this dispersion would be and what scale limit should be considered. Thinking about several nearby agglomeration points, so that some clusters of TiO_2 can be present in different positions thus making the whole process more effective, may not be a problem. The presence of different, close enough, cluster sizes of TiO_2, so that when one of these spots finishes working, there is still another one to receive the wavelength and start the activation again, can make the system even more effective.

Considering the concept of pixelated network, each pixel would be a cluster of TiO_2 connected by a TiO_2 wire forming a magnetic mesh, so that the wavelength reached each pixel (TiO_2 cluster) and made the network swing. The wavelength can be imagined as a ball, and the TiO_2, with various particle sizes, forming a network that holds this ball, as shown in Fig. 21 (a, b). If the net is punctured or fragmented, the ball will pass through the hole without touching (vibration), and therefore, without activating the net, as shown in Fig. 21 (c, d).

The focus should not be on whether the network is composed by nano- or microparticles but on the composition between all these scales creating connections, in which smaller particles, with higher surface area and therefore more likely to agglomerate, would be used as clusters, while larger particles, with smaller surface area and easier dispersion, would be used as the wires that would provide the connections between clusters, thus contributing to the better formation of the functional cake cover and activation of TiO_2 particles.

A study performed by Suh et al. [23], through the elementary mapping of Ti using EDX in SEM images of TiO_2/CO_3-LDH, has revealed that the distribution of TiO_2 based on CO_3-LDH is in the aggregate form. The scale seen in the author's research indicates clusters of TiO_2 up to 700 nm. Thus, for the nanoscale network proposed, TiO_2 needs to present an agglomeration as naturally

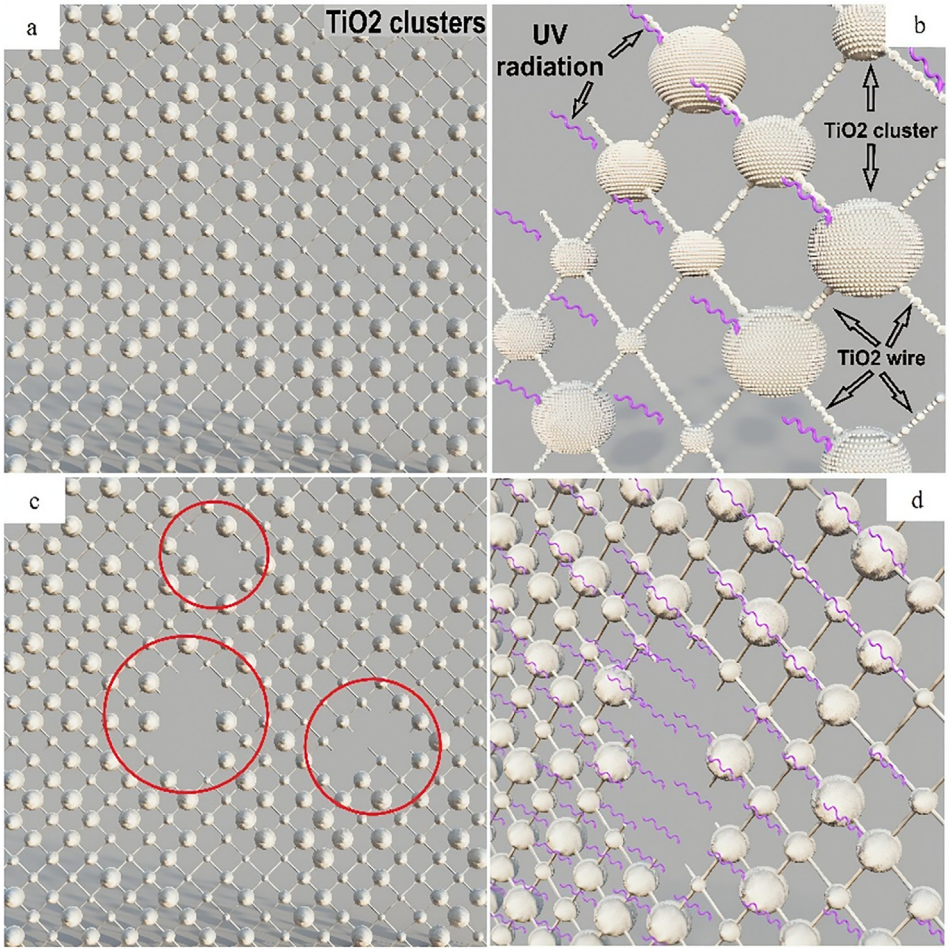

Fig. 21. Example of TiO_2 pixelated network forming a magnetic mesh.

observed by the authors, which would not be difficult given the various particle sizes sold in the market and which would allow UV radiation to activate all the different TiO_2 particles present in the system.

Dantas, Vittorino, and Loh [20] have observed the formation of clusters of TiO_2 in whiter areas in the surface of mortar specimens, which suggests that they were more active and that the TiO_2 present in the other areas of the mortar was not so effective probably because these areas were completely covered by pollution particles and not activated, and therefore, the dirt particle did not degrade and the specimens had no self-cleaning.

As a result, taking into account that the issue of network formation and dispersion is a function of the distribution of the particle size of TiO_2 in a dry state before being added, the use of TiO_2 powder could be an alternative if this product presents a large distribution of particle sizes of TiO_2, which would provide greater chances in the network's formation with no particle size having high predominance in a restrict distribution range. Thereby, the concept of interparticle separation (IPS) for TiO_2 becomes a topic to be observed as the dimensions of particles are useful to understand whether they would allow the formation of cake cover.

4.3. UV radiation light and TiO_2 particles

Reflectance measurement processes allow the observation of the activation of TiO_2 when the angle of UV light incidence occurs directly on surfaces. However, in this condition, the micro- and nano-roughness of the surface can have a shading effect on TiO_2 particles and therefore impair the total activation of TiO_2.

Considering macro-roughness, light reflection can be better understood and worked. However, at the nano- and micro-roughness levels, which need further studies, the direction of light reflection changes greatly and can difficult the activation of TiO_2. Parkins ([24] apud [15]) also includes a reflection coefficient that depends on the surface inclination, where close together points on the surface give rise to the diffuse signal, while points on the surface contribute to the specular signal.

Solar energy distribution between direct and diffuse radiation is necessary for the activation of TiO_2. If direct radiation could cause higher activation of TiO_2 due to more energy, it is necessary to think that because of the existence of nano- and micro-roughness, there is the effect of micro-shading of the TiO_2 particles according to the sun path, as well as the irradiation of the surface only for a few hours of the day. On the other hand, diffuse radiation, despite the lower energy, can irradiate the surface for many hours, and still eliminate the effect of micro-shading, since it will radiate on the surface from all sides.

In other words, the existence of an extremely rough surface, in addition to causing a high index of micro-shading due to peaks and valleys, allows great dirt adhesion. Under this condition, diffuse radiation plays a fundamental role in the activation of TiO_2, as it allows valleys to be unaffected by the shadows of the peaks since diffuse radiation would come from anywhere. Therefore, the question to be answered is whether diffuse radiation has enough energy to enable the activation of TiO_2 when the numerous surface interactions are considered.

The relationship between direct and diffuse solar radiation is variable throughout the day, and in the first hours of the day, this relationship is almost 1/1. Whereas UV is a small fraction of this ratio, the radiation rate used by TiO_2 in photocatalytic processes should be considered. The TiO_2 absorbs radiation in the UV range of 315–380 nm, and the anatase crystalline phase has a range of 3.2 eV corresponding to a wavelength of approximately 380 nm, while the rutile crystalline phase has a range of 3.0 eV, which corresponds to a wavelength of 413 nm [25].

Although radiation with a wavelength below 380 nm can excite the electrons of the valence band (BV) to the conduction band (BC) of the material, the TiO_2 that has a more extensive commercial application absorbs in the UV range only approximately 3%–5% of the solar energy that reaches the terrestrial surface. This way, TiO_2 does not take advantage of all the solar radiation incident in the photocatalytic processes [25–27].

Considering that at noon in São Paulo (Brazil) the total solar radiation is $\approx \mathbf{1.8 \times 10^{25}}$ **eV**, it is known that only 5% of this amount corresponds to the UV required in the activation of TiO_2, therefore an energy of $\approx \mathbf{9.0 \times 10^{23}}$ **eV**. Taking as a reference the lowest rate of absorption of TiO_2 (3%), TiO_2 absorbs an energy of $\approx \mathbf{2.7 \times 10^{22}}$ **eV**. Thus, judging by these values and considering that the activation energy of TiO_2 is in the order of a few eV (3.0 eV and 3.2 eV), it is possible to perceive that the diffused solar radiation energy in the early hours of the day will be enough to promote the activation of TiO_2, which makes diffuse radiation, in these cases, as or more important than direct radiation, since regardless of the surface roughness, it will allow the activation of TiO_2 for long periods of the day, as shown in Figs. 22 and 23, if the TiO_2 particles are not shaded by pollution particles, as shown in Figs. 19 and 20.

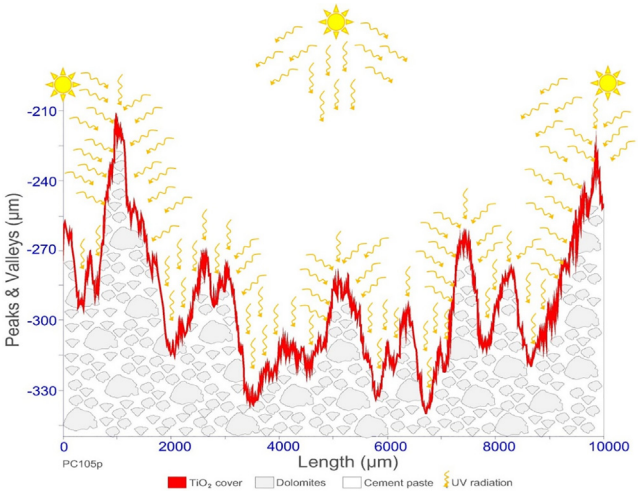

Fig. 22. Example of activation of cake cover by UV radiation on the measured micro-roughness of the mortar sample with addition of TiO_2.

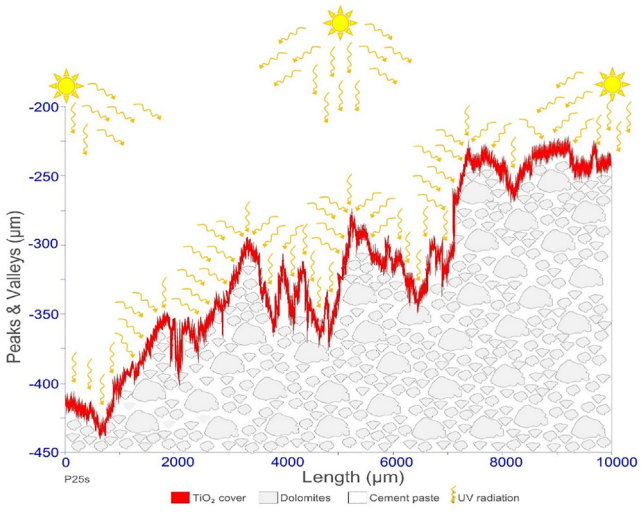

Fig. 23. Example of activation of cake cover by UV radiation on the measured micro-roughness of the mortar sample with suspension of TiO_2.

As with many theories for the interaction of waves with rough surfaces, it is assumed that any part of the incident beam interacts only once with the surface before being spread. However, even if there is a finite possibility that, for certain directions of the energy of the scattered waves, a second interaction or additional interactions with the surface may occur, this will not interfere in the activation of TiO_2, as, given the energy needed for the activation of TiO_2, the numerous light interactions will not cause any damage to its activation, regardless of TiO_2 treatments added or applied as a suspension.

Consequently, it is still necessary to consider that in both TiO_2 treatments, added or applied as a suspension, pollution particles can shade the TiO_2 particles at the valleys and limit its activation. Thus, for the activation of TiO_2 and its effectiveness in the photocatalytic process in rough surfaces, it is necessary to investigate the interaction of TiO_2 in the nano- and micrometric scales and its dispersion process in these surfaces. Moreover, the effect of solar radiation incident beam must be considered in these particles and surfaces. Then, the largest number of active particles in the surface must be obtained to provide better efficiency for the system.

A practical approach that could be evaluated by the building industry, whether with the use of TiO_2 in powder or suspension, would be the care with the TiO_2 mixture when added to the cementitious matrix, providing better dispersion of the compound. Regarding the suspension care, the production and finishing surface is essential to achieve a good covering and thus allowing a greater activation and maintenance of the photocatalytic activity over time.

5. Conclusions and remarks

This study describes an approach for evaluating how the microscale roughness affects the distribution of TiO_2 and contributes to the adhesion of pollution particles, which affects the activation of TiO_2 by solar radiation. The main findings can be summarized as follows:

- Activation of TiO_2 is not limited only to direct solar radiation, with diffuse solar radiation being as or more important because of the longer surface irradiation time;
- Micro-roughness has no direct relationship with the activation of TiO_2. However, it can supply a higher adhesion to dirt and prevent the activation of TiO_2;
- The presence of different roughness scales and the use of the same TiO_2 particle size affect the process of dispersion of TiO_2 in surfaces;
- Different TiO_2 particle sizes can help in the formation of the TiO_2 pixelated network and enhance its activation, thus providing a better system efficiency;
- The use of suspension of TiO_2 does not guarantee better effectiveness, since the formation of an imperfect film layer in the surface, caused by a deficient application or the characteristics of the TiO_2 particles used, reduces UV radiation and consequently system efficiency;

The outcomes highlighted how the microscale roughness cannot be considered advantageous when exploited in relation of the adhesion to dirt and consequence non activation of TiO_2 by solar radiation. Thus, considering that in the angstrom and nanoscales different interaction mechanisms are involved in tribological processes [16], the possibility of tribological processes impacting the dispersion of TiO_2 particles should be studied, as well as their influence on the self-cleaning process.

Tribology is a nanoscale issue that can affect the agglomeration of TiO_2; this agglomeration is causally linked of the formation of TiO_2 clusters, which in turn can also be impacted by the particle size distribution of the formation of TiO_2 pixelated network. Thus, based on this theory, about the TiO_2 producer, what suggests is to increase the range of the particle size of TiO_2 should be increased from 1 μm to 80 μm instead of 20 μm to 30 μm to achieve a more efficient TiO_2 pixelated mesh, and the discussion could reach the level that the presence of TiO_2 clusters is not exactly a photocatalysis problem, but rather it can help the entire process.

On the other hand, this opens the space to discuss that changing TiO_2 powder by suspension of TiO_2 may not be an advantage. If at first, the suspension applied to the surfaces may present a better performance concerning self-cleaning, its useful life is certainly shorter than in mortar with TiO_2 since it does not allow the change in film layer without a new suspension application.

CRediT authorship contribution statement

Sérgio Roberto Andrade Dantas: Conceptualization, Methodology, Investigation, Software, Writing - original draft. **Roberto Cesar de Oliveira Romano:** Writing - review & editing. **Fúlvio Vittorino:** Writing - review & editing, Supervision. **Kai Loh:** Writing - review & editing, Supervision.

Declaration of Competing Interest

The authors declare that they have no known competing financial interests or personal relationships that could have appeared to influence the work reported in this paper.

Acknowledgements

The authors wish to thank the Institute of Technological Research (IPT) and its foundation (FIPT) for the financial and institutional support through the New Talents Program N° 01/2017. To the Coordenação de Aperfeiçoamento de Pessoal de Nível Superior - Brazil (CAPES) - Finance Code 001 for the financial support and the Laboratory of Microstructure and Material Eco-efficiency (LME). In the same way to thank to Cristal Pigmentos do Brasil for the material support and the support of all technicians to this research work.

References

[1] R.S. Dariani, A. Esmaeili, A. Mortezaali, S. Dehghanpour, Photocatalytic reaction and degradation of methylene blue on TiO_2 nano-sized particles, Optik 127 (2016) 7143–7154.
[2] D. Feng, N. Xie, C. Gong, Z. Leng, H. Xiao, H. Li, X. Shi, Portland cement paste modified by TiO_2 nanoparticles: a microstructure perspective, Ind. Eng. Chem. Res. 52 (2013) 11575–11582.
[3] D.L. Liao, B.Q. Liao, Shape, size and photocatalytic activity control of TiO_2 nanoparticles with surfactants, J. Photochem. Photobiol., A 187 (2007) 363–369.
[4] D.L. Liao, G.S. Wu, B.Q. Liao, Zeta potential of shape-controlled TiO_2 nanoparticles with surfactants, Colloids Surf., A 348 (2009) 270–275.
[5] A.H.P. de Oliveira, J.A.S. Moura, H.P.de. Oliveira, Preparação e Caracterização de Microfibras de Poli (Álcool Vinílico) / Dióxido de Titânio. Polímeros, Instituto de Pesquisa em Ciência dos Materiais, Universidade Federal do Vale do São Francisco – UNIVASF. Juazeiro, 2012.
[6] P. Munafò, G.B. Goffredo, E. Quagliarini, TiO_2-based nanocoatings for preserving architectural stone surfaces: an overview, Constr. Build. Mater. 84 (2015) 201–218.
[7] L. Pinho, M.J. Mosquera, Photocatalytic activity of TiO_2–SiO_2 nanocomposites applied to buildings: influence of particle size and loading, Appl. Catal. B 134–135 (2013) 205–221.
[8] H.D. Jang, S. Kim, Effect of particle size and phase composition of titanium dioxide on photocatalytic properties, J. Nanoparticles Res. 3 (2001) 141–147.
[9] J. Wade, An investigation of TiO-ZnFe O Nanocomposites for visible light photocatalysis. Master Thesis. University of South Florida, Department of Electrical Engineering. 108p. 2005.

[10] R. Levinson, P. Berdahl, H. Akbari, Solar spectral optical properties of pigments— Part II: survey of common colorants, Solar Energy Materials & Solar Cells, v.89, p.351-389, 2005.
[11] R. Levinson, P. Berdahl, H. Akbari, Solar spectral optical properties of pigments—Part I: model for deriving scattering and absorption coefficients from transmittance and reflectance measurements, Solar Energy Materials & Solar Cells, 89 (2005) 319–349.
[12] L. Senff, J.A. Labrincha, V.M. Ferreira, D. Hotza, W.L. Repette, Effect of nano-silica on rheology and fresh properties of cement pastes and mortars. Construction and Building Materials, 23 (2009) 2487–2491.
[13] L. Senff, D. Hotza, W.L. Repette, V.M. Ferreira, J.A. Labrincha, Effect of nanosílica and microsílica on the microstructure and the hardened properties of cement pastes and mortars. Adv. Appl. Ceram. 109 (2010) 104–110.
[14] G. Husken, M. Hunger, H.J.H. Brouwers, Experimental study of photocatalytic concrete products for air purification, Build. Environ. 44 (2009) 2463–2474.
[15] J.A. Ogilvy, Wave scattering from rough surfaces, Rep. Prog. Phys. 50 (1987) 1553–1608.
[16] F.M. Borodich, A. Pepelyshev, O. Savencu, Statistical approaches to description of rough engineering surfaces at nano and microscales, Tribol. Int. 103 (2016) 197–207.
[17] C.Y. Poon, R.S. Saylest, T.A. Jones, Surface measurement and fractal characterization of naturally fractured rocks, J. Phys. D Appl. Phys. 25 (1992) 1269–1275.
[18] S.R.A. Dantas, R. Serafini, R.C.de.O. Romano, F. Vittorino, K. Loh, Influence of the nano TiO_2 dispersion procedure on fresh and hardened rendering mortar properties, Constr. Build. Mater. 215 (2019) 544–556.
[19] ABNT, NBR 14656: Portland cement and raw materials - Chemical analysis by X-ray spectrometry – Test method, Rio de Janeiro (2001) [in Portuguese].
[20] S.R.A. Dantas, F. Vittorino, K. Loh, Photocatalytic Performance of White Cement Mortars Exposed in Urban Atmosphere, Global Journal of Researches in Engineering: C (Chemical Engineering), 19 (2) version 1 (2019) 1–13.
[21] Z. Chen, Y. Liu, P. Zhou, A comparative study of fractal dimension calculation methods for rough surface profiles, Chaos, Solitons Fractals 112 (2018) 24–30.
[22] J.A. Ogilvy, J.R. Foster, Rough surfaces: gaussian or exponential statistics? Journal of Physics D: Applied Physics, 32 (2015) 1243–1251, 1989. Springer, 418.
[23] M.-J. Suh, Y. Shen, C.K. Chan, J.-H. Kim, Titanium Dioxide Layered Double Hydroxide Composite Material for Adsorption-Photocatalysis of Water Pollutants, Langmuir, 2019. DOI: 10.1021/acs.langmuir.9b00539
[24] B.E. Parkins, J. Acoust. Soc. Am. 41 (1967) 126–134.
[25] J. de Dios, J.M. del Campo, D. Colorado, Decontamination through photocatalytic TiO2 additions. Past, Present and Future. 2nd International Conference on Emerging Trends in Engineering and Technology (icetet'2014), May 30-31, 2014 London (united Kingdom), [s.l.], p.145-152, 30 May 2014. International Institute of Engineers. http://dx.doi.org/10.15242/iie.e0514557.
[26] A. Mills, S.L. Hunte, An overview of semiconductor photocatalysis, J. Photochem. Photobiol., A 108 (1997) 1–35.
[27] D. Li, H. Huang, X. Chen, Z. Chen, W. Li, D. Ye, X. Fu, New synthesis of excellent visible-light TiO2–xNx photocatalyst using a very simple method, J. Solid State Chem. 180 (2007) 2630–2634.